PHYSICAL REVIEW B **89**, 081304(R) (2014)

Spin noise spectroscopy of a single quantum well microcavity

S. V. Poltavtsev,[1] I. I. Ryzhov,[1] M. M. Glazov,[1,2] G. G. Kozlov,[1] V. S. Zapasskii,[1] A. V. Kavokin,[1,3] P. G. Lagoudakis,[3] D. S. Smirnov,[2] and E. L. Ivchenko[2]

[1]*Spin Optics Laboratory, St. Petersburg State University, 1 Ul'anovskaya, Peterhof, St. Petersburg 198504, Russia*

[2]*Ioffe Physical-Technical Institute of the RAS, 26 Polytekhnicheskaya, St. Petersburg 194021, Russia*

[3]*School of Physics and Astronomy, University of Southampton, SO17 1 BJ, Southampton, United Kingdom*

(Received 27 November 2013; revised manuscript received 23 January 2014; published 10 February 2014)

We report on an experimental observation of spin noise in a single semiconductor quantum well embedded into a microcavity. The great cavity-enhanced sensitivity to fluctuations of optical anisotropy has allowed us to measure the Kerr rotation and ellipticity noise spectra in the strong-coupling regime. The spin noise spectra clearly show two resonant features: a conventional magnetoresonant component shifting towards higher frequencies with a magnetic field and an unusual "nonmagnetic" component centered at zero frequency and getting suppressed with an increasing magnetic field. We attribute the first of them to the Larmor precession of free electron spins, whereas, the second one is presumably due to hyperfine electron-nuclei spin interactions.

DOI: 10.1103/PhysRevB.89.081304 PACS number(s): 72.25.Rb, 71.36.+c, 72.70.+m, 78.47.−p

Introduction. In the present-day physics of semiconductor nanostructures, considerable interest is shown for the fundamental spin-related properties which are also promising in applications. Among optical methods of spin dynamics studies, an important place is given to the Faraday-rotation-based spin noise (SN) spectroscopy (SNS), which became well known and popular during the past several years [1]. The advantages of SNS are primarily owed to its nonperturbative nature because probing the sample response by a weak laser beam in the region of transparency does not lead to any real electronic transitions. Extreme smallness of the magnetization fluctuations detected with the SNS technique calls for the highest polarimetric sensitivity, which is achieved by using various electronic or optical means. A real breakthrough occurred when the fast-Fourier-transform (FFT) spectrum analyzers were applied in electronics of the SNS technique [2]. The most straightforward optical way to enhance the polarimetric sensitivity implies increasing intensity of the probe light beam and, simultaneously, leaving the input power of the photodetector on the admissible level. This can be implemented either by using high-extinction polarization geometries [3] or by placing the sample inside a high-Q optical cavity [4]. In both cases, the light power density on the sample can be increased by a few orders of magnitude with the light power on the photodetector and, therefore, the photocurrent shot noise remaining on the same low level.

For low-dimensional semiconductor structures (quantum wells, wires, and dots), the problem of polarimetric sensitivity is especially topical. In Ref. [5], in order to increase the signal, the spin noise spectra of n-doped GaAs quantum wells were studied in the samples containing ten identical quantum wells (QWs). The measurement of the spin noise spectrum of a layer of InAs/GaAs quantum dots (QDs) in a high-finesse microcavity allowed Dahbashi *et al*. [6] to perform a unique investigation of spin dynamics of a single heavy hole localized in a selected QD. We experimentally study the spin noise in a single quantum well here.

In this Rapid Communication, we report on an observation of spin noise in a single GaAs QW embedded inside a high-finesse microcavity operating in the strong-coupling regime. A dramatic increase in the sensitivity has made it possible to observe, in addition to the Kerr rotation fluctuations, the noise of ellipticity, the effect reported previously for atomic gases only [7]. We also demonstrate that an increase in the probe beam intensity from weak to moderate values significantly perturbs the spin system in the microcavity making it possible to study the spin noise in steady nonequilibrium states as well [8–10].

Experiment. The sample under study represents a 20-nm GaAs QW with AlAs barriers grown along the $z \parallel [001]$ axis, placed into the λ cavity formed by two distributed Bragg mirrors composed of 25 and 15 pairs of AlAs/AlGaAs layers. Two additional narrow 2.6-nm QWs were grown on both sides of the central well, which enabled us to use photodoping by means of the above-barrier illumination. The sample had a gradient of thickness that made it possible to vary the detuning by moving the light spot on the sample. The structure is described in more detail in Ref. [11]. The schematic of the sample and its reflection spectra are presented in Figs. 1(a) and 1(b), respectively. The reflection spectra under our experimental conditions of cw excitation were somewhat smoother than those presented in Ref. [11] but still allowed one to trace anticrossings of the cavity mode with material excitations of the QW, namely, the negatively charged trion (X^-), heavy- (X_{hh}), and light-hole (X_{lh}) excitons. The observation of trion resonance means electron density n_e not to be higher than $\sim 5 \times 10^{10}$ cm^{-2}, see Ref. [11] for details. The sample was placed at a temperature of about 6 K into a small transverse magnetic field $B = 0 \cdots 30$ mT (Voigt geometry), and the fluctuations of the polarization plane rotation were detected in the reflection geometry (Kerr rotation noise) using a standard setup with a balanced photoreceiver (bandwidth of 200 MHz) and a FFT spectrum analyzer, see Ref. [1] for details. The signal of ellipticity noise was also measured by placing a properly oriented quarter-wave plate in front of the balanced detector. The probe light from a tunable cw Ti:sapphire laser was tightly focused on the sample (diameter of the spot was ~ 20 μm) and was tuned to the cavity resonance at the chosen point of the sample. In some cases, the probed area of the sample was additionally illuminated by a laser diode with a

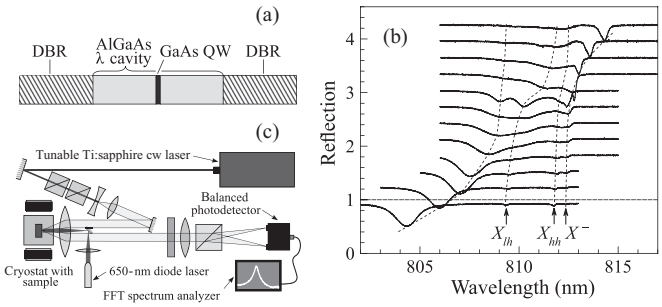

FIG. 1. (a) Schematic of the sample. (b) Reflection spectra measured at different points of the sample, i.e., at different detunings. Arrows mark the positions of negative trion (X^-), heavy-hole (X_{hh}), and light-hole (X_{lh}) resonances. Different curves are shifted along the vertical axis for clarity. Dotted lines are guides for eye and demonstrate anticrossings. (c) Schematic of the experimental setup.

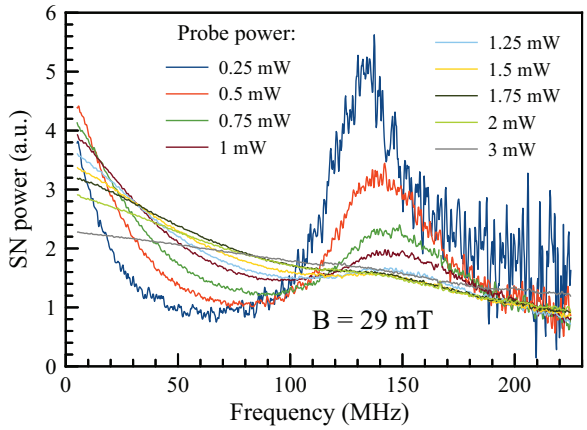

FIG. 3. (Color online) Spin noise power density extracted from the total Kerr rotation noise by normalizing the signal-to-noise ratio by the probe power measured at $B = 29$ mT and $T = 3.6$ K.

shorter wavelength of ∼650 nm and a power density of about 25 mW/cm^2. A schematic of the experimental setup is shown in Fig. 1(c).

Under the above experimental conditions, in most cases, the Kerr rotation and ellipticity noise were comparable to or even exceeded the shot-noise level so that the noise signals could be easily detected. At the same time, these signals were spatially inhomogeneous with a typical length scale of about 100 μm. Specifically, depending on the particular area of the sample, the spin noise signals could also be observed in the absence, rather than only in the presence, of the additional short-wavelength illumination. In this Rapid Communication, we restrict ourselves to systematic results obtained in our studies of SN spectra of the system at the negative photon-exciton detuning with the cavity mode lying below the exciton and trion resonances. The dependence of the signals on the magnetic field and probe power was similar in different spots of the sample.

Experimental results. Figure 2 demonstrates (a) Kerr rotation noise and (b) ellipticity noise at negative detuning from the X_{hh} resonance $\delta \approx -2.8$ meV. At the chosen point, the noise was observed only under additional illumination. The noise spectrum has been found to contain generally two resonant features with essentially different sensitivities to the applied magnetic field. The frequency of one of them, as expected for a spin resonance, linearly varied with the field (this component is termed magnetic hereafter), whereas, the other peak centered at zero frequency did not exhibit any shift with the applied field ("nonmagnetic" component). As seen from Fig. 2, the nonmagnetic feature decreases in amplitude with increasing the magnetic field. Moreover, the amplitudes and widths of both components depend strongly on the probe beam intensity as illustrated in Fig. 3. Particularly, with the decrease in the probe intensity, both magnetic and nonmagnetic resonances narrow down, and the relative magnitude of the magnetic resonance increases making it possible to observe the field-dependent component of spin noise in the pure form.

Figure 4(a) presents the Kerr rotation noise spectra at different transverse magnetic fields measured without above-barrier illumination at the sample point where the magnetic component is most pronounced. A field-induced shift in the magnetic component corresponded to the effective g factor equal to $|g| \approx 0.33$, which correlates with the electron g-factor value in the 20-nm GaAs QW [12]. The shape of this resonance can be well approximated by a field-independent Lorentzian with a FWHM of 60 MHz corresponding to the dephasing time

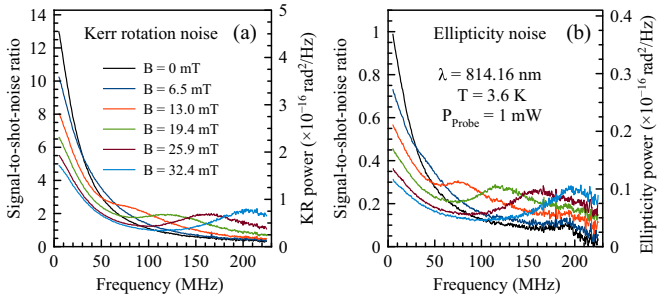

FIG. 2. (Color online) (a) Kerr rotation and (b) ellipticity noise spectra measured at fixed probe power and different magnetic fields indicated in the legend. Shot noise is subtracted from the data, and the signals are normalized to the shot-noise level (see Ref. [17] for details of the normalization). The right-hand axis shows the Kerr rotation noise power in rad^2/Hz.

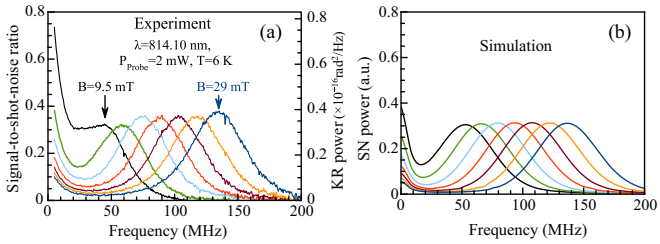

FIG. 4. (Color online) (a) Measured Kerr rotation noise spectra for the magnetic field varied from 9.5 to 29 mT in equal steps. Parameters of the experiment are given in the panel. (b) Calculated spin noise power spectra for $g = -0.33$, $\tau_s \approx 24$ ns, and $\delta_e \approx 1.9 \times 10^8$ s^{-1}(≈30 MHz). The 7% spread in electron g-factor values is taken into account, see Refs. [13,17] for details.

of 6 ns. The narrow peak at zero frequency can be attributed to the hyperfine interaction with lattice nuclei [13]. Its width of about 15 MHz corresponds to the spin relaxation time of $\tau_s = 25$ ns. Overall, such a behavior of the experimental data is well reproduced theoretically as shown in Fig. 4(b), see below for details.

Discussion. The noise of Kerr rotation and ellipticity is caused by the fluctuations in reflection coefficients $r_\pm$ of the microcavity for right (+) and left (−) circularly polarized components of the probe beam. If the probe frequency ω is close to the cavity resonance frequency ω_c, the reflection coefficients can be presented as [14,15]

$$r_\pm = -1 + \frac{i\varkappa_1}{\omega - \omega_c + i\frac{\varkappa_1+\varkappa_2}{2} + \sum_j \frac{g^2_{j,\pm}}{\omega-\omega_{j,\pm}+i\gamma_{j,\pm}}}. \qquad (1)$$

Here, $\varkappa_1$ and $\varkappa_2$ are the photon escape rates through the mirrors (light is incident on the mirror characterized by $\varkappa_1$), j enumerates resonances in the active layer, namely, the X^- trion and X_{hh}, X_{lh} excitons, $\omega_{j,\pm}$ are the corresponding resonance frequencies, and $g_{j,\pm}$ and $\gamma_{j,\pm}$ are the coupling constants and damping rates, respectively. In general, the differences $\omega_{j,+} - \omega_{j,-}$, $g_{j,+} - g_{j,-}$, and $\gamma_{j,+} - \gamma_{j,-}$ are proportional to the z component of magnetization in the system, making the instant values r_+ and r_- different [16]. As follows from Eq. (1), the reflection coefficient, as a function of the probe frequency, has dips at the resonant frequencies of mixed modes or polaritons [Fig. 1(b)]. We assume that the main contribution to the Kerr rotation and ellipticity fluctuations results from the spin noise of the resident electrons and, thus, we take into account only trion resonance. In this case, the fluctuations in the trion oscillator strength cause the fluctuating splitting of polariton resonance for σ^+ and σ^- polarizations. As a result, the ellipticity noise $\propto |r_+|^2 - |r_-|^2$ should reveal two peaks at the slopes of the resonance and should vanish in its center where $|r_+|^2 = |r_-|^2$, whereas, Kerr rotation noise, governed by the phase of the reflection coefficient, should be peaked at the resonance center. This is demonstrated in Fig. 5 where the experimental data and calculated optical spectra are shown in panels (a) and (b), respectively, see Ref. [17] for details.

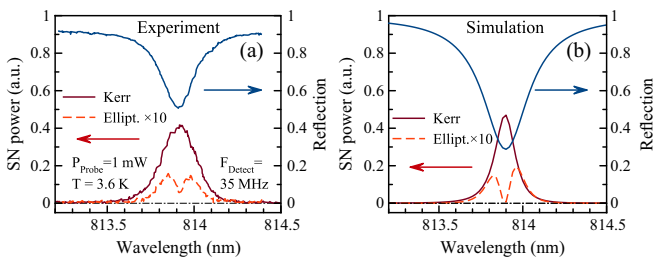

FIG. 5. (Color online) (a) Reflectivity (top blue curve, right axis), Kerr rotation (solid/dark red), and ellipticity (dashed/red) optical spectra. (b) Results of the calculation after Eq. (1) for $\hbar\omega_c = 1523.52$ meV (wavelength of 813.8 nm), $\hbar\varkappa_1 = 0.5$, and $\hbar\varkappa_2 = 0.14$ meV, taking into account only X^- resonance with $\hbar\omega_{X^-} = 1526.9$ meV (812 nm), $\hbar g_{X^-} = 0.8$, and $\hbar\gamma_{X^-} = 0.1$ meV, and taking into account the inhomogeneous broadening 0.8 meV of the trion resonance [17].

Strong sensitivity of the spin noise spectra on the probe intensity, particularly, the effects of probe light on amplitudes and widths of the magnetic and nonmagnetic components in the spin noise spectra, clearly demonstrates that, in the strongly coupled quantum microcavity, even a moderate probe perturbs the system. Such a nonequilibrium system calls for special theoretical treatment. The unambiguous presence of the magnetic component demonstrates that the noise of Kerr rotation and ellipticity can be attributed to the spin fluctuations in resident electrons, which can be present in the structure due to unintentional doping and/or above-barrier illumination. For relatively low electron densities $n_e \sim 10^{10}$ cm^{-2}, the carriers are localized at QW imperfections, and their spins are affected by both the external magnetic field $\boldsymbol{B}$ and the nuclear field fluctuations. In the strong-coupling regime, the probe beam, even detuned from material resonances, generates exciton-polaritons and trion-polaritons in the structure. Here, we consider the simplest model, which takes into account: (i) the precession of a localized electron spin in the nuclear field fluctuation with frequency $\boldsymbol{\Omega}_N$, which is randomly distributed as $\mathcal{F}(\boldsymbol{\Omega}_N) = (\sqrt{\pi}\delta_e)^3 \exp(-\Omega_N^2/\delta_e^2)$ with δ_e being the nuclear spin fluctuation [13], (ii) the effect of external magnetic field $\boldsymbol{B}$ with the Larmor frequency $\boldsymbol{\Omega}_B = g\mu_B B/\hbar$, and (iii) probe-induced coupling of electrons and trions neglecting a contribution from excitons. The coupled dynamics of electron and trion spins is described by [16,18]

$$\frac{d\boldsymbol{S}}{dt} = (\boldsymbol{\Omega}_N + \boldsymbol{\Omega}_B) \times \boldsymbol{S} - \frac{\boldsymbol{S}}{\tau_s} - G\boldsymbol{S} + \frac{S_T \boldsymbol{e}_z}{\tau_0^T}, \qquad (2a)$$

$$\frac{dS_T}{dt} = -\frac{S_T}{\tau_T} + GS_z. \qquad (2b)$$

Here, $\boldsymbol{S}$ is the electron spin pseudovector with the components S_x, S_y and S_z, S_T is the trion pseudospin $S_T = (T_+ - T_-)/2$ with $T_\pm$ being the occupation numbers of heavy-hole trions with spins 3/2 and −3/2, respectively, $\boldsymbol{e}_z$ is the unit vector along the growth axis z, τ_s is the electron spin relaxation time and, for simplicity, the effects of spin relaxation anisotropy related to crystallographic orientation of the quantum well are disregarded [19], τ_0^T is the lifetime of the trion, τ_T is the spin lifetime of the trion given by $\tau_s^T \tau_0^T/(\tau_s^T + \tau_0^T)$ with τ_s^T being the trion spin relaxation time, and G is the trion generation rate. The latter includes the formation of trions both directly by the probe absorption and via the capture of excitons by resident electrons, and it is proportional to the probe intensity and increases with decreasing absolute value of the detuning $|\delta|$. The spin precession in the trion is neglected. We stress that, for the linearly polarized probe, the trions, thus created, contain electrons with any spin orientation, but, according to the optical selection rules, the electron, returned after the trion recombination, has a spin $\boldsymbol{S} = S_T \boldsymbol{e}_z$.

Figure 4(b) demonstrates the calculation of the electron spin noise spectra $(\delta S_z^2)_\omega$ by using Eqs. (2) in the limit of low probe intensity $G \to 0$. The parameters of the calculation are given in the caption. The model reproduces the main features of measured spin noise spectra, Fig. 4 (a): the narrow peak at $\omega = 0$, which vanishes with the increase in the field, and the magnetic peak.

An increase in probe intensity and, hence, the trion generation rate G drastically changes the spin noise spectra as

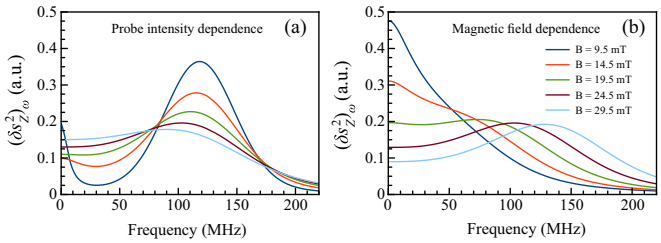

FIG. 6. (Color online) Calculated spin noise spectra. (a) Different curves correspond to different trion generation rates $G = 0 \cdots 5 \times 10^8$ s^{-1} (in equal steps), and the magnetic field is fixed $B = 24$ mT. (b) Different curves correspond to different magnetic fields $B = 9.5 \cdots 29.5$ mT (in equal steps), and the generation rate is fixed $G = 4 \times 10^8$ s^{-1}. Other parameters are as follows: $\tau_0^T = 11$ ps, $\tau_T = 9.5$ ps, and $\delta_e = 2.5 \times 10^8$ s^{-1}, and the spread of g-factor values is disregarded.

shown in Fig. 6. In qualitative agreement with the experimental data presented in Fig. 3, the magnetic peak in the spin noise spectrum decreases, whereas, the peak at $\omega = 0$ becomes broader and relatively more pronounced. Such a behavior can be qualitatively understood bearing in mind that the probe-induced coupling of the electron with the trion leads to the anisotropic spin relaxation of the electron. Indeed, at $\tau_s^T \gg \tau_0^T$, the electron spin z component is conserved, whereas, its in-plane components S_x and S_y vanish after the trion decay. As a result, the electron effective spin relaxation rate γ_{eff} increases with the field giving rise to the broadening of the spin noise spectrum [5]. Calculation shows that, for $G\tau_T \ll 1$, $\Omega_B < G\tau_T/(2\tau_0^T)$ and in the absence of random nuclear fields [17],

$$\gamma_{\text{eff}} = \frac{1}{\bar{T}} - \frac{G}{2}\sqrt{\frac{\tau_T^2}{{\tau_0^T}^2} - \frac{4\Omega_B^2}{G^2}}, \tag{3}$$

where $\bar{T}^{-1} = 1/\tau_s + G[1 - \tau_T/(2\tau_0^T)]$. It follows then that, for small enough magnetic fields, the spin noise spectrum is centered at $\omega = 0$ and its width increases quadratically with the magnetic field. For $\Omega_B > G\tau_T/(2\tau_0^T)$, the magnetic component in the spin noise spectrum appears. The simulation after Eqs. (2) presented in Figs. 6(a) and 6(b) reproduces well not only the magnetic-field dependence of the spin noise spectrum, shown in Fig. 2 and measured at the moderate probe intensity, but also the dependence of the spin noise spectrum on the probe intensity Fig. 3.

A detailed fitting of the experimental data by the developed model needs allowance for other possible sources of the nonmagnetic component of the spin noise spectrum, e.g., spin fluctuations of holes (in the generated trions or captured in the sample as a result of above-barrier illumination), spin noise of excitons [20] and exciton-polaritons [9], and spin noise of electrons and holes trapped in narrow quantum wells or at the localization centers in the barriers. Additionally, the nonmagnetic component of the ellipticity noise can result from fluctuations in the off-diagonal component of the background dielectric susceptibility tensor $\text{Re}\{\varepsilon_{xy}\}$, caused, e.g., by the phonons. To elucidate the contributions of particular mechanisms, the application of magnetic field in the Faraday geometry, which enhances the hyperfine-interaction-induced zero-frequency peak could be useful [6,13,21,22]. All these effects are, however, beyond the scope of the present Rapid Communication and deserve further study.

Conclusion. The electron spin noise in a single QW microcavity operating in the strong-coupling regime is observed via the Kerr rotation and ellipticity fluctuations. The spin noise spectrum contains both a magnetic component, with its maximum located at the frequency of Larmor precession of the electron spin around the external magnetic field, and a nonmagnetic one centered at zero frequency. The magnitudes and widths of these components strongly depend on the probe intensity. The experimental findings are described in the framework of the proposed model, which takes into account the spin precession of resident electrons in the external magnetic field and the field of nuclear fluctuations as well as the effect of trion generation by the probe beam.

Acknowledgments. Financial support from the Russian Ministry of Education and Science (Contract No. 11.G34.31.0067 with SPbSU and leading scientist A. V. Kavokin), Dynasty Foundation, RFBR, and EU projects POLAPHEN and SPANGL4Q is acknowledged. A partial support from the SkolTech/MIT Initiative is acknowledged. The work was fulfilled using the equipment of SPbSU resource center "Nanophotonics."

[1] V. S. Zapasskii, Adv. Opt. Photon. **5**, 131 (2013).
[2] M. Romer, J. Hubner, and M. Oestreich, Rev. Sci. Instrum. **78**, 103903 (2007).
[3] P. Glasenapp, A. Greilich, I. I. Ryzhov, V. S. Zapasskii, D. R. Yakovlev, G. G. Kozlov, and M. Bayer, Phys. Rev. B **88**, 165314 (2013).
[4] A. V. Kavokin, M. R. Vladimirova, M. A. Kaliteevski, O. Lyngnes, J. D. Berger, H. M. Gibbs, and G. Khitrova, Phys. Rev. B **56**, 1087 (1997).
[5] G. M. Müller, M. Römer, D. Schuh, W. Wegscheider, J. Hübner, and M. Oestreich, Phys. Rev. Lett. **101**, 206601 (2008).
[6] R. Dahbashi, J. Hübner, F. Berski, K. Pierz, and M. Oestreich, arXiv:1306.3183.
[7] T. Mitsui, Phys. Rev. Lett. **84**, 5292 (2000).
[8] E. L. Ivchenko, Fiz. Tverd. Tela **7**, 1489 (1974) [Sov. Phys. Solid State **7**, 998 (1974)].
[9] M. M. Glazov, M. A. Semina, E. Y. Sherman, and A. V. Kavokin, Phys. Rev. B **88**, 041309 (2013).
[10] F. Li, Y. V. Pershin, V. A. Slipko, and N. A. Sinitsyn, Phys. Rev. Lett. **111**, 067201 (2013).
[11] R. Rapaport, E. Cohen, A. Ron, E. Linder, and L. N. Pfeiffer, Phys. Rev. B **63**, 235310 (2001).
[12] I. A. Yugova, A. Greilich, D. R. Yakovlev, A. A. Kiselev, M. Bayer, V. V. Petrov, Y. K. Dolgikh, D. Reuter, and A. D. Wieck, Phys. Rev. B **75**, 245302 (2007).
[13] M. M. Glazov and E. L. Ivchenko, Phys. Rev. B **86**, 115308 (2012).

[14] D. F. Walls and G. J. Milburn, *Quantum Optics*, 2nd ed. (Springer, Berlin, 2008).
[15] C. Y. Hu, A. Young, J. L. O'Brien, W. J. Munro, and J. G. Rarity, Phys. Rev. B **78**, 085307 (2008).
[16] M. M. Glazov, Phys. Solid State **54**, 1 (2012).
[17] See Supplemental Material at http://link.aps.org/supplemental/10.1103/PhysRevB.89.081304 for details.
[18] G. V. Astakhov, M. M. Glazov, D. R. Yakovlev, E. A. Zhukov, W. Ossau, L. W. Molenkamp, and M. Bayer, Semicond. Sci. Technol. **23**, 114001 (2008).
[19] N. S. Averkiev and L. E. Golub, Phys. Rev. B **60**, 15582 (1999).
[20] D. S. Smirnov, M. M. Glazov, and E. L. Ivchenko (unpublished).
[21] The effect of the magnetic field in the Faraday geometry on spin noise spectra was addressed theoretically in Ref. [13] and experimentally in Refs. [6,22]. Such an experimental geometry is not possible in our setup.
[22] Y. Li, N. Sinitsyn, D. L. Smith, D. Reuter, A. D. Wieck, D. R. Yakovlev, M. Bayer, and S. A. Crooker, Phys. Rev. Lett. **108**, 186603 (2012).